Article | Received 20 February 2025; Accepted 30 June 2025; Published 23 July 2025
https://doi.org/10.55092/ae20250003

Double-channel event-triggered adaptive tracking control of nonstrict-feedback nonlinear systems with separate state transmission

Yingjie Deng[1,2], Fangcheng Liu[2], Yifei Xu[1,2,*], Fubo Li[2], Tao Ni[1,2] and Dingxuan Zhao[1,2]

[1] State Key Laboratory of Crane Technology, Yanshan University, Qinhuangdao 066004, China

[2] School of Mechanical Engineering, Yanshan University, Qinhuangdao 066004, China

* Correspondence author; E-mail: xyf@ysu.edu.cn.

Highlights:

- Taking advantage of the bounded characteristic of fuzzy basis functions, the proposed scheme includes merely one adaptive law in each step of the virtual control laws.
- The devised virtual control laws are not involved in the final control input but presented for the analysis use. This train of thought can unite the event-triggered control (ETC) design in both channels and solve the jumps of virtual control laws (JVCL) problem flexibly.
- The proposed separate transmission principle ensures the effective utilization of the unoccupied channel in the inter-event time. In comparison to the conventional event-triggered mechanism, the communication bandwidth is significantly decreased.

Abstract: This paper proposes an event-triggered tracking control scheme of the nonstrict-feedback nonlinear systems working in both sensor-to-controller (SC) and controller-to-actuator (CA) channels. Aiming at the problems of "algebraic loop" and "jumps of virtual control laws (JVCL)" arising in the backstepping-based event-triggered control (ETC), this paper incorporates the bounded property of basis functions of fuzzy logic systems (FLS) to direct adaptive control, and puts forward a novel method through fabricating undetermined virtual control laws. To utilize the unoccupied communication channel produced by ETC, this paper raises a novel ETC working mechanism called "separate state transmission". Not like traditional ETC, the states herein are not transmitted in a cluster, which avoids the huge occupancy of network at the triggering instant. The separation is achieved by constructing a cumulative triggering condition. Under the assumption of the compact set of states, it proves all the tracking and estimation errors are ultimately bounded. Simulation verifies the feasibility of the entire work.

Keywords: double-channel event-triggered control (ETC); nonstrict-feedback nonlinear system; jumps of virtual control laws (JVCL); separate state transmission

1. Introduction

Many industrial plants can be described by a mathematical model of nonstrict-feedback nonlinear systems, such as the ball and beam system, the coupled turning and heeling model of vehicles, and the multiple link manipulator. Moreover, the controller of a nonstrict-feedback nonlinear systems keeps it downward compatibility to some other generic systems like strict-feedback systems and pure-feedback systems, which are deemed as special cases. As a recursive design procedure based on elementary Lyapunov analysis, backstepping has shown its talent for nonlinear control. Associated with artificial intelligence of FLS and neural networks (NNs), adaptive fuzzy and neural backstepping control was commonly shown in existing works to deal with uncertainties, see [1] for the command-filtered backstepping of large-scale systems, [2] for the fault-tolerant control of switched systems, [3] for the optimized backstepping of strict-feedback systems, and [4] for the dynamic surface control of strict-feedback systems. In view of the nonstrict-feedback nonlinear system, the "algebraic loop" problem should be addressed in the backstepping design, which implies the synchronous variation of virtual control laws along with the states. In [5–7], the variable separation principle was proposed, which decomposed the nonlinearity into the combination of tracking errors. In [8–10], the "algebraic loop" problem was offset by using the bounded property of the fuzzy basis functions. In [11,12], two-level NNs were constructed to accomplish the state recovery and control together. In [13], the "algebraic loop" problem was circumvented due to the stationary property of states in the inter-event time of ETC. To list some recent advanced techniques to control nonstrict-feedback nonlinear systems, [14] introduced the asymptotic tracking control to the stochastic nonstrict-feedback nonlinear system; [15] dealt with the asymmetric time-varying constraint of the output by using asymmetric Lyapunov function; [16] combined the C^1 finite-time control with the logarithm barrier Lyapunov function; [17] proposed an event-triggered fixed-time control scheme. As we have learnt, the disposal of the "algebraic loop" problem is no longer the main concern in recent researches.

Traditional continuous control may cause the jam of communication traffic, which facilitates the technique of ETC [18–20]. The intermittent sampling of signals employed in this technique is capable of effectively conserving communication resources. Event-triggered mechanism can function in two channels, namely the SC channel and the CA channel. Generally, In an industrial plant, the quantity of sensors exceeds that of actuators. Thus, ETC in the SC channel has significant merit than it in the CA channel. In [21–25] and many existing works, ETC in the SC channel was designed for diverse systems. Nevertheless, all of the concerned systems can be transformed to the affine nonlinear system or the first-order linear model. For the high-order nonlinear systems including the nonstrict-feedback system like [15,17,26–28], it is observed that most of researches only cover the ETC in the CA channel. Since the backstepping method is commonly used to construct control laws, the updating of states at triggering instants will inevitably cause the virtual control law to jump abruptly, a phenomenon termed the JCVL problem in [29,30]. The JVCL problem was neglected in some ETC in the SC channel, such as [31,32]. However, this disposal could incur the instability and was not rigorous in mathematics. In [13,29,30], the JCVL problem was addressed by constructing filters, which generated the continuous substitutes for discontinuous virtual control laws. In [33], this problem was solved by using the controller in the form of NN. Nevertheless, these works were presented with strict parameter selection and stability analysis.

It is acknowledged that the advantage of ETC is to reduce communication traffic. The inter-event time between two triggering instants supplied extra space for signal transmission. However, the existing researches seldom considered the reuse of this space. For the above mentioned ETC, all the sampled signals were transmitted in a cluster at the triggering instants, which required more bandwidth for communication. For example, if the ETC is designed for the n-order system in the SC channel, there are n states required to be transmitted at each triggering instant. In this light, we are conceiving of a novel event-triggered mechanism in a limited bandwidth, in which the states are separately transmitted according to the triggering condition. The saved channels in the inter-event time can be used for transmission of the other states. Thus, n states can be transmitted through the bandwidth of 1 state.

Motivated by the above challenges, this paper investigates the ETC of nonstrict-feedback nonlinear systems in both the SC and the CA channels, in which the states are separately transmitted by sharing a mutual SC channel with the bandwidth of 1 state. The "algebraic loop" problem is solved by fabricating the adaptive laws approximating the norms of fuzzy weights. The JVCL problem is released by proposing a novel method called undetermined virtual control laws. The separation of state transmission is achieved by constructing the cumulative triggering condition. Compared with the existing works, contributions of this paper can be concluded as

(1) By using the bounded property of fuzzy basis functions, the proposed scheme only contains one adaptive law in each step of virtual control laws, which is more succinct than [8,11,14].
(2) The devised virtual control laws are not involved in the final control input but presented for the analysis use. This train of thought can unite the ETC design in both channels and solve the JCVL problem flexibly. Compared with the single-channel ETC like [27,29], the proposed double-channel ETC can save more communication resources. Compared with [13,33], the JVCL problem is solved in an easier way.
(3) The proposed separate transmission principle ensures the effective utilization of the unoccupied channel in the inter-event time. In comparison to the conventional event-triggered mechanism, the communication bandwidth is largely reduced.

2. Preliminaries

Consider the following nonstrict-feedback nonlinear system

$$\begin{aligned} \dot{x}_i &= x_{i+1} + f_i(x) + d_i,\ i = 1, \cdots, n-1 \\ \dot{x}_n &= u + f_n(x) + d_n \\ y &= x_1 \end{aligned} \tag{1}$$

where x_i is the state and $x = [x_1, \cdots, x_n]^{\mathrm{T}}$, $f_i(x)$ is the unknown model dynamics and d_i is the exogenous disturbance in each subsystem, u is the control input, and y is the output. To ensure the controllability, the following assumptions are preset

Assumption 1. *All states are defined within a compact set, specifically denoted as* $\Omega_x = \{x | x^{\mathrm{T}} x \leq \Delta\}$ *and* $\Delta > 0$. $f_i(x)$ *and* $f_n(x)$ *exhibit boundedness when* $x \in \Omega_x$. $|d_i|$ *is bounded, with its upper bound remaining unknown.*

Assumption 2. *[11]* $f_i(x)$ *must not include any linear component of* x_{i+1}*, that is,* $f_i(x) = b_i x_{i+1} + g_i(x)$

and b_i is a constant.

Remark 1. *It is evident that the control will malfunction when $b_i = -1$ in Assumption 2. As will be utilized in the subsequent analysis, the universal approximation theorem pertaining to the FLS is stated as follows.*

Lemma 1. *[10] Any continuous function $f(x)$ within a compact can be represented by a FLS, taking the form $f(x) = W^{\mathrm{T}}\varphi(x) + \varepsilon(x)$. Here, $\varepsilon(x)$ stands for the approximation error, which is bounded such that $|\varepsilon(x)| \leq \bar{\varepsilon}$, $W = \arg\min_{W_f \in U}\{\bar{\varepsilon}\}$ refers to the vector of fuzzy weights where U is a compact set of W_f, and $\varphi(x)$ denotes the vector of fuzzy basis functions. Based on the definition of $\varphi(x)$, an important property is known that $\varphi(x)^{\mathrm{T}}\varphi(x) \leq 1$.*

The control objective is to present the control law of u with the event-triggered sampling of x_i separately, so that y is able to track the reference signal y_d. y_d is required to have the first-order continuous derivative of $\dot{y}_d$.

3. Control design

The control framework associated with the proposed scheme is depicted in Figure 1. By separately acquiring the state of x_i and ξ_i at the triggering instant t_{j^i} where $j^i = 1, 2, \cdots, +\infty$, the controller can generate the command control law v. By acquiring v at the triggering instant t_j^u, u is finally obtained. During the inter-event time $t \in (t_{j^i}, t_{j^i+1}]$ and $t \in (t_{j^u}, t_{j^u+1}]$, $\xi_i(t_{j^i})x_i(t_{j^i})$ and $v(t_{j^u})$ are held by zero-order holders (ZOHs).

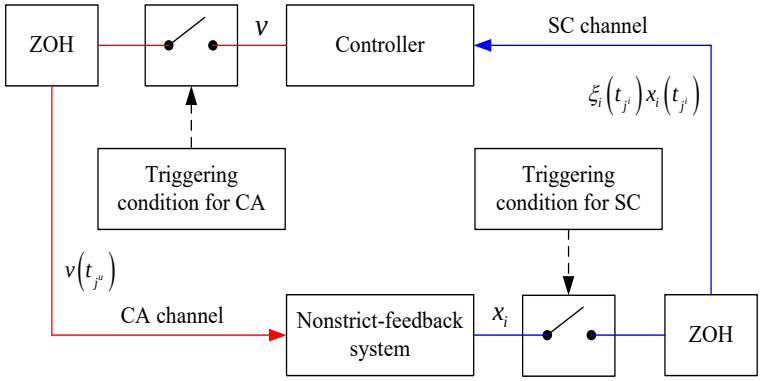

Figure 1. Control framework.

Before the ETC design, the continuous backstepping control is presented as the basis, which is carried out according to following steps.

Step 1: The virtual control law in the subsystem of $\dot{x}_1$ is designed as

$$\alpha_1 = -k_1 z_1 - \frac{\hat{\theta}_1}{2b_1} z_1 \tag{2}$$

where $k_1 > 0$ and $b_1 > 0$ are tuning parameters, and $z_1 = y - y_d$ denotes the tracking error. $\hat{\theta}_1$ is the adaptive parameter to be designed later.

The tracking error is $z_i = x_i - \alpha_{i-1}$ for $i = 2, \cdots, n$. According to Lemma 1, we can fabricate a FLS as

$$f_1(x) + d_1 - \dot{y}_d = W_1^{\mathrm{T}}\varphi_1(s_1) + \varepsilon_1(s_1) \tag{3}$$

where $s_1 = [x^{\mathrm{T}}, d_1, \dot{y}_d]^{\mathrm{T}}$ and $|\varepsilon_1(s_1)| \leq \bar{\varepsilon}_1$. By differentiating z_1 along with (1)–(3) and $x_2 = z_2 + \alpha_1$, it renders

$$\dot{z}_1 = -k_1 z_1 - \frac{\hat{\theta}_1}{2b_1} z_1 + W_1^{\mathrm{T}} \varphi_1(s_1) + \varepsilon_1(s_1) + z_2 \tag{4}$$

According to the Young's inequality and $\varphi_1^{\mathrm{T}}(s_1)\varphi_1(s_1) \leq 1$, it is known that

$$W_1^{\mathrm{T}} \varphi_1(s_1) z_1 \leq \frac{W_1^{\mathrm{T}} W_1}{2b_1} z_1^2 + \frac{b_1}{2}$$
$$\varepsilon_1(s_1) z_1 \leq \frac{z_1^2}{2} + \frac{\bar{\varepsilon}_1^2}{2}$$

Define $\theta_1 = W_1^{\mathrm{T}} W_1$ and $\tilde{\theta}_1 = \theta_1 - \hat{\theta}_1$. Design the adaptive law of $\hat{\theta}_1$ as

$$\dot{\hat{\theta}}_1 = \frac{\lambda_1}{2b_1} z_1^2 - \sigma_1 \hat{\theta}_1 \tag{5}$$

where $\lambda_1 > 0$ and $\sigma_1 > 0$ are two tuning parameters.

Select the Lyapunov candidate as $V_1 = z_1^2/2 + \tilde{\theta}_1^2/(2\lambda_1)$. Differentiating V_1 along with (4) and (5), it renders

$$\begin{aligned} \dot{V}_1 &\leq -k_1 z_1^2 + z_1 z_2 + \frac{\tilde{\theta}_1}{2b_1} z_1^2 + \frac{b_1}{2} + \frac{z_1^2}{2} + \frac{\bar{\varepsilon}_1^2}{2} - \frac{1}{\lambda_1} \tilde{\theta}_1 \dot{\hat{\theta}}_1 \\ &\leq -(k_1 - 1) z_1^2 - \frac{\sigma_1}{2\lambda_1} \tilde{\theta}_1^2 + \frac{z_2^2}{2} + \frac{b_1}{2} + \frac{\bar{\varepsilon}_1^2}{2} + \frac{\sigma_1}{2\lambda_1} \theta_1^2 \end{aligned} \tag{6}$$

Step i ($2 \leq i \leq n-1$): The virtual control law within the subsystem of $\dot{x}_i$ is designed as

$$\alpha_i = -k_i z_i - \frac{\hat{\theta}_i}{2b_i} z_i \tag{7}$$

where $k_i > 0$ and $b_i > 0$ are two tuning parameters.

According to Lemma 1, we can fabricate a FLS as

$$f_i(x) + d_i - \dot{\alpha}_{i-1} = W_i^{\mathrm{T}} \varphi_i(s_i) + \varepsilon_i(s_i) \tag{8}$$

where $s_i = [x^{\mathrm{T}}, d_1, \cdots, d_i, y_d, \dot{y}_d, \hat{\theta}_1, \cdots, \hat{\theta}_{i-1}]^{\mathrm{T}}$ and $|\varepsilon_i(s_i)| \leq \bar{\varepsilon}_i$. Recursively, we can render

$$\dot{\alpha}_{i-1} = \frac{\partial \alpha_{i-1}}{\partial y_d} \dot{y}_d + \sum_{j=1}^{i-1} \left(\frac{\partial \alpha_{i-1}}{\partial x_j} \dot{x}_j + \frac{\partial \alpha_{i-1}}{\partial \hat{\theta}_j} \dot{\hat{\theta}}_j \right)$$

By differentiating z_i along with (1), (7) and (8), it renders

$$\dot{z}_i = -k_i z_i - \frac{\hat{\theta}_i}{2b_i} z_i + W_i^{\mathrm{T}} \varphi_i(s_i) + \varepsilon_i(s_i) + z_{i+1} \tag{9}$$

According to the Young's inequality and $\varphi_i^{\mathrm{T}}(s_i)\varphi_i(s_i) \leq 1$, it is known that

$$W_i^{\mathrm{T}} \varphi_i(s_i) z_i \leq \frac{W_i^{\mathrm{T}} W_i}{2b_i} z_i^2 + \frac{b_i}{2}$$
$$\varepsilon_i(s_i) z_i \leq \frac{z_i^2}{2} + \frac{\bar{\varepsilon}_i^2}{2}$$

Define $\theta_i = W_i^{\mathrm{T}} W_i$ and $\tilde{\theta}_i = \theta_i - \hat{\theta}_i$. Design the adaptive law of $\hat{\theta}_i$ as

$$\dot{\hat{\theta}}_i = \frac{\lambda_i}{2b_i} z_i^2 - \sigma_i \hat{\theta}_i \tag{10}$$

where $\lambda_i > 0$ and $\sigma_i > 0$ are two tuning parameters.

Select the Lyapunov candidate as $V_i = z_i^2/2 + \tilde{\theta}_i^2/(2\lambda_i)$. Differentiating V_i along with (9) and (10), it renders

$$\begin{aligned}\dot{V}_i \leq & -k_i z_i^2 + z_i z_{i+1} + \frac{\tilde{\theta}_i}{2b_i} z_i^2 + \frac{b_i}{2} + \frac{z_i^2}{2} + \frac{\bar{\varepsilon}_i^2}{2} - \frac{1}{\lambda_i}\tilde{\theta}_i\dot{\hat{\theta}}_i \\ \leq & -(k_i - 1)z_i^2 - \frac{\sigma_i}{2\lambda_i}\tilde{\theta}_i^2 + \frac{z_{i+1}^2}{2} + \frac{b_i}{2} + \frac{\bar{\varepsilon}_i^2}{2} + \frac{\sigma_i}{2\lambda_i}\theta_i^2\end{aligned} \tag{11}$$

Step n: The virtual control law in the subsystem of $\dot{x}_n$ is designed as

$$\alpha_n = -k_n z_n - \frac{\hat{\theta}_n}{2b_n} z_n \tag{12}$$

where $k_n > 0$ and $b_n > 0$ are two tuning parameters.

According to Lemma 1, we can fabricate a FLS as

$$f_n(x) + d_n - \dot{\alpha}_{n-1} = W_n^{\mathrm{T}}\varphi_n(s_n) + \varepsilon_n(s_n) \tag{13}$$

where $s_n = [x^{\mathrm{T}}, d_1, \cdots, d_n, y_d, \dot{y}_d, \hat{\theta}_1, \cdots, \hat{\theta}_n]^{\mathrm{T}}$ and $|\varepsilon_n(s_n)| \leq \bar{\varepsilon}_n$, and it has

$$\dot{\alpha}_{n-1} = \frac{\partial \alpha_{n-1}}{\partial y_d}\dot{y}_d + \sum_{j=1}^{n-1}\left(\frac{\partial \alpha_{n-1}}{\partial x_j}\dot{x}_j + \frac{\partial \alpha_{n-1}}{\partial \hat{\theta}_j}\dot{\hat{\theta}}_j\right)$$

Differentiating z_n along with (1), (12) and (13), it renders

$$\dot{z}_n = -k_n z_n - \frac{\hat{\theta}_n}{2b_n} z_n + u - \alpha_n + W_n^{\mathrm{T}}\varphi_n(s_n) + \varepsilon_n(s_n) \tag{14}$$

According to the Young's inequality and $\varphi_n^{\mathrm{T}}(s_n)\varphi_n(s_n) \leq 1$, it is known that

$$\begin{aligned}W_n^{\mathrm{T}}\varphi_n(s_n) z_n \leq & \frac{W_n^{\mathrm{T}} W_n}{2b_n} z_n^2 + \frac{b_n}{2} \\ \varepsilon_n(s_n) z_n \leq & \frac{z_n^2}{2} + \frac{\bar{\varepsilon}_n^2}{2}\end{aligned}$$

Define $\theta_n = W_n^{\mathrm{T}} W_n$ and $\tilde{\theta}_n = \theta_n - \hat{\theta}_n$. Design the adaptive law of $\hat{\theta}_n$ as

$$\dot{\hat{\theta}}_n = \frac{\lambda_n}{2b_n} z_n^2 - \sigma_n \hat{\theta}_n \tag{15}$$

where $\lambda_n > 0$ and $\sigma_n > 0$ are two tuning parameters.

Select the Lyapunov candidate as $V_n = z_n^2/2 + \tilde{\theta}_n^2/(2\lambda_n)$. Differentiating V_n along with (14) and (15), it renders

$$\begin{aligned}\dot{V}_n \leq & -k_n z_n^2 + (u - \alpha_n) z_n + \frac{\tilde{\theta}_n}{2b_n} z_n^2 + \frac{b_n}{2} + \frac{z_n^2}{2} + \frac{\bar{\varepsilon}_n^2}{2} - \frac{1}{\lambda_n}\tilde{\theta}_n\dot{\hat{\theta}}_n \\ \leq & -(k_n - \frac{1}{2})z_n^2 - \frac{\sigma_n}{2\lambda_n}\tilde{\theta}_n^2 + \frac{b_n}{2} + \frac{\bar{\varepsilon}_n^2}{2} + \frac{\sigma_n}{2\lambda_n}\theta_n^2 + (u - \alpha_n) z_n\end{aligned} \tag{16}$$

Remark 2. *It is clear from (2), (5), (7), (10), (12) and (15) that the system follows from the traditional continuous control if $u = \alpha_n$. In this case, all the tracking and estimation errors are ultimately bounded by adding up $V_1, \cdots, V_n$. To be combined with the ETC, the influence of $u - \alpha_n$ on the stability will be analyzed.*

Define $k_i' = k_i + \hat{\theta}_i/(2b_i)$ for $i = 1, \cdots, n$. According to (2) and (7), (12) can be finally transformed to

$$\alpha_n = -[k_n' x_n + k_n' k_{n-1}' x_{n-1} + \cdots + k_n' \cdots k_1' (x_1 - y_d)] \tag{17}$$

Define $\xi_i = k_n' \cdots k_i'$. (17) can be further written as

$$\alpha_n = -\sum_{i=1}^{n} \xi_i x_i + \xi_1 y_d \tag{18}$$

It is observed from (18) that the final control law can be divided by the components of x_i and y_d.

Considering the SC channel, the command control law v is designed as

$$v = -\sum_{i=1}^{n} \xi_i(t_{j^i}) x_i(t_{j^i}) + \xi_1(t_{j^y}) y_d(t_{j^y}) \tag{19}$$

where t_{j^y} is the triggering instant of y_d and $j^y = 1, \cdots, +\infty$. Here, (19) holds for $t \in (t_{j^i}, t_{j^i+1}]$ and $t \in (t_{j^y}, t_{j^y+1}]$.

Define $e_i = |\xi_i x_i - \xi_i(t_{j^i}) x_i(t_{j^i})|$ and $e_y = |\xi_1 y_d - \xi_1(t_{j^y}) y_d(t_{j^y})|$. The separate transmission of $\xi_i x_i$ and $\xi_1 y_d$ is achieved by constructing the triggering condition in the SC channel as

$$\begin{aligned} t_{j^i+1} &= \{t > t_{j^i} | \sum_{i=1}^{n} e_i + e_y \geq \mu_v \wedge e_i = \max[e_1, \cdots, e_n, e_y]\} \\ t_{j^y+1} &= \{t > t_{j^y} | \sum_{i=1}^{n} e_i + e_y \geq \mu_v \wedge e_y = \max[e_1, \cdots, e_n, e_y]\} \end{aligned} \tag{20}$$

where $\mu_v > 0$ is the constant triggering threshold.

Remark 3. *If there are more than one x_i and y_d satisfying (20) at the same time, we only need to select one of them randomly and update the corresponding t_{j^i+1}.*

Remark 4. *The proposed train of thought "undetermined virtual control laws" implies that the virtual control laws (2), (7) and (12) are not involved in the control command (19) but only constructed for the analytical use. Thus, there is no need to analyze the discontinuity of virtual control laws at the triggering instants, such that the JVCL problem is solved.*

Considering the CA channel, we can further design

$$u = v(t_{j^u}),\ t \in (t_{j^u}, t_{j^u+1}] \tag{21}$$

Define $e_u = |u - v|$. The triggering condition in the CA channel is designed as

$$t_{j^u+1} = \{t > t_{j^u} | e_u \geq \mu_u\} \tag{22}$$

where $\mu_u \geq 2\mu_v$ is the constant triggering threshold.

Lemma 2. *Under the Assumption 1, the proposed triggering conditions (20) and (22) can ensures the minimum inter-event times in both SC and CA channels, namely no "Zeno" behavior.*

Proof: Denote the minimum inter-event times as $\tau_i = \min\{t_{j^i+1} - t_{j^i}\}$, $\tau_y = \min\{t_{j^y+1} - t_{j^y}\}$ and $\tau_u = \min\{t_{j^u+1} - t_{j^u}\}$. It is clear that $e_i = 0$, $e_y = 0$ and $e_u = 0$ at t_{j^i}, t_{j^y} and t_{j^u} respectively. From the definition of e_i and e_y, it is known that

$$\dot{e}_i = |\dot{\xi}_i x_i + \xi_i \dot{x}_i| = \left| \sum_{j=i}^{n} \frac{\partial \xi_i}{\partial \hat{\theta}_j} (\frac{\lambda_j}{2b_j} z_j^2 - \sigma_j \hat{\theta}_j) x_i + \xi_i (x_{i+1} + f_i(x) + d_i) \right| \tag{23}$$

and

$$\dot{e}_y = |\dot{\xi}_1 y_d + \xi_1 \dot{y}_d| = \Big| \sum_{j=1}^{n} \frac{\partial \xi_1}{\partial \hat{\theta}_j} (\frac{\lambda_j}{2b_j} z_j^2 - \sigma_j \hat{\theta}_j) y_d + \xi_1 \dot{y}_d \Big| \tag{24}$$

According to Assumption 1, it is known from (23) and (24) that $\dot{e}_i$ and $\dot{e}_y$ are bounded. Define $c_i \geq \dot{e}_i$ and $c_y \geq \dot{e}_y$. Invoking (20), it is easily inferred that

$$\tau_i \geq \frac{\mu_v}{c_i(n+1)}, \ \tau_y \geq \frac{\mu_v}{c_y(n+1)} \tag{25}$$

τ_i and τ_y only concern the minimum inter-event times of the same x_i and y_d. The minimum inter-event time between two adjacent triggering instants (either for the same variable or the different) is marked as τ_m. It is inferred from the implications of (20) that (26) holds at the triggering instant $t_{j^i}^+$.

$$\mu_v - \sum_{i=1}^{n} e_i - e_y \geq \frac{\mu_v}{n+1} \tag{26}$$

Because we cannot make sure which x_i and y_d will be updated at the next triggering instant, it is reasonable that

$$\tau_m \geq \frac{\mu_v}{(n+1)(\sum_{i=1}^{n} c_i + c_y)} \tag{27}$$

Because v is a discontinuous value in (19), we cannot get $\dot{v}$. Denote the latest triggering instant in the SC channel after t_{j^u} as t_m, namely for all $j^i = 1, \cdots, +\infty$ and $j^y = 1, \cdots, +\infty$.

$$t_m = \{t > t_{j^u} | t - t_{j^u} = \min[t_{j^i} - t_{j^u}, t_{j^y} - t_{j^u}]\} \tag{28}$$

We can infer from (20) that $|v(t_m^+) - u| \leq \mu_v$ and $|v(t_{m+1}) - v(t_m^+)| \leq \mu_v$, where t_{m+1} denotes the latest triggering instant of v in $t > t_m$. Thus, it can be further inferred from the definition of e_u that

$$\begin{aligned} e_u(t_{m+1}) =& |v(t_{m+1}) - u| \\ \leq& |v(t_{m+1}) - v(t_m^+)| + |v(t_m^+) - u| \leq 2\mu_v \end{aligned} \tag{29}$$

Invoking $\mu_u \geq 2\mu_v$, $t_{m+1} - t_m \geq \tau_m$ and $t_m - t_{j^u} > 0$, it is inferred from (22) that

$$\tau_u = \min\{t_{j^u+1} - t_{j^u}\} \geq t_{m+1} - t_{j^u} \geq t_{m+1} - t_m \geq \tau_m \tag{30}$$

See (25), (27) and (30), the proof is completed.

4. Stability analysis

The proposed scheme is concluded in the following theorem.

Theorem 1. *Under the Assumption 1 and Assumption 2, the proposed ETC scheme of (19) and (21) with the triggering conditions (20) and (22) can guarantee that all z_i and $\tilde{\theta}_i$ in the nonstrict-feedback nonlinear system of (1) are ultimately bounded by selecting appropriate tuning parameters.*

Proof: It is inferred from the triggering conditions of (20) and (22) that

$$|u - \alpha_n| \leq |u - v| + |v - \alpha_n| \leq e_u + \sum_{i=1}^{n} e_i + e_y \leq \mu_v + \mu_u \tag{31}$$

By substituting (31) to (16) and using the Young's inequality, it renders

$$\begin{aligned}\dot{V}_n \leq & -k_n z_n^2 + (u-\alpha_n)z_n + \frac{\tilde{\theta}_n}{2b_n} z_n^2 + \frac{b_n}{2} + \frac{z_n^2}{2} + \frac{\bar{\varepsilon}_n^2}{2} - \frac{1}{\lambda_n}\tilde{\theta}_n\dot{\hat{\theta}}_n \\ \leq & -(k_n - \frac{3}{2})z_n^2 - \frac{\sigma_n}{2\lambda_n}\tilde{\theta}_n^2 + \frac{b_n}{2} + \frac{\bar{\varepsilon}_n^2}{2} + \frac{\sigma_n}{2\lambda_n}\theta_n^2 + \frac{\mu_v^2}{2} + \frac{\mu_u^2}{2}\end{aligned} \tag{32}$$

Select the Lyapunov candidate as $V = \sum_{i=1}^{n} V_i$. The derivative of V can be rendered by adding up (6), (11) and (32).

$$\begin{aligned}\dot{V} \leq & -(k_1 - 1)z_1^2 - \sum_{i=2}^{n-1}(k_i - \frac{3}{2})z_i^2 - (k_n - 2)z_n^2 \\ & - \sum_{i=1}^{n}\frac{\sigma_i}{2\lambda_i}\tilde{\theta}_i^2 + \sum_{i=1}^{n}(\frac{b_i}{2} + \frac{\bar{\varepsilon}_i^2}{2} + \frac{\sigma_i}{2\lambda_i}\theta_i^2) + \frac{\mu_v^2}{2} + \frac{\mu_u^2}{2}\end{aligned} \tag{33}$$

Select $k_1 > 1$, $k_i > 3/2$ and $k_n > 2$. Define $\eta = \min\{2k_1 - 2, 2k_i - 3, 2k_n - 4, \sigma_i\}$ and $\rho = \sum_{i=1}^{n}(b_i/2 + \bar{\varepsilon}_i^2/2 + \sigma_i\theta_i^2/(2\lambda_i)) + \mu_v^2/2 + \mu_u^2/2$. Then, (33) can be simplified as

$$\dot{V} \leq -\eta V + \rho \tag{34}$$

It is inferred from (34) that $V(t) \leq V(0)\exp(-\eta t) + \rho/\eta(1 - \exp(-\eta t))$. Because $z_i \leq \sqrt{2V}$ and $\tilde{\theta}_i \leq \sqrt{2\lambda_i V}$, it is inferred that z_i is ultimately bounded by $\sqrt{2\rho/\eta}$ and $\tilde{\theta}_i$ is ultimately bounded by $\sqrt{2\lambda_i\rho/\eta}$. The proof is completed.

Remark 5. *From the definitions of η and ρ in (34), it is known that the ultimate bound of the tracking error z_i will be tuned down by increasing k_1, k_i, k_n, σ_i and λ_i as well as decreasing b_i, μ_v and μ_u. However, this tuning will increase the control cost, lead to the bad tracking transient and decrease the inter-event time. Thus, the tuning principle of all the parameters should follow from the satisfactory control performance.*

5. Simulation analysis

For the purpose of verifying the effectiveness of the proposed scheme, the following 3-order system is presented for the test.

$$\begin{aligned}\dot{x}_1 =& x_2 + 2x_3 - x_2\sin(x_1)\cos(x_3) - 2 + d_1 \\ \dot{x}_2 =& x_3 + x_1 + x_3\cos(x_2) + d_2 \\ \dot{x}_3 =& u + \ln(2 + x_1^2 + x_2^2 + x_3^2) + d_3\end{aligned} \tag{35}$$

where $d_1 = 0.1\sin(2\pi t/5)$, $d_2 = 0.1\sin(\pi t/5)$ and $d_3 = 0.1\sin(4\pi t)$. The reference signal is set as $y_d = 2\sin(2\pi t/5)$.

Three schemes are compared in the simulation. The first one is the proposed double ETC with separate state transmission, which is marked as "DETC-ST". The parameters are set with

$$\begin{aligned}& k_1 = k_3 = 20, k_2 = 1, b_1 = b_2 = b_3 = 10, \\ & \lambda_1 = 0.8, \lambda_2 = \lambda_3 = 0.01, \sigma_1 = \sigma_2 = \sigma_3 = 0.5, \\ & \mu_v = 10, \mu_u = 20\end{aligned} \tag{36}$$

The second scheme is the ETC in the SC channel with clustered state transmission, which is marked as "ETC-CT". The control input in this scheme is devised as

$$u = -\sum_{i=1}^{n} \xi_i(t_j)x_i(t_j) + \xi_1(t_j)y_d(t_j) \tag{37}$$

where t_j denotes the triggering instant of signal transmission. The triggering condition is devised as

$$t_{j+1} = \{t > t_j || u - \alpha_n| \geq \mu_v\} \tag{38}$$

The tuning parameters of this scheme follow from (44). The third scheme is the ETC without considering the "JVCL" problem, which stems from and is marked as "ETC-WJ". The control laws in this scheme are designed as

$$\begin{aligned} \alpha_1 &= -k_1 z_1' - \hat{\theta}_1 z_1' \\ \alpha_i &= -k_i z_i' - \hat{\theta}_i z_i', \ i = 2, \cdots, n-1 \\ u &= -k_n z_n' - \hat{\theta}_n z_n' \end{aligned} \tag{39}$$

where $z_1' = x_1(t_j) - y_d$, $z_i' = x_i(t_j) - \alpha_{i-1}(t_j^+)$ and $z_n' = x_n(t_j) - \alpha_{n-1}(t_j^+)$. Define $e_i = x_i - x_i(t_j)$ for $i = 1, \cdots, n$, $e = [e_1, \cdots, e_n]^{\mathrm{T}}$ and $z' = [z_1', \cdots, z_n']^{\mathrm{T}}$. The triggering condition is designed as

$$t_{j+1} = \{t > t_j | \|e\| \geq \kappa \|z\|\} \tag{40}$$

where κ is set as 0.085. The update law of $\hat{\theta}_i$ in this scheme is set as

$$\begin{aligned} \hat{\theta}_i(t_j^+) &= 0.1\hat{\theta}_i(t_j) + \frac{0.5e_i}{e_i^2 + 1}, \ t = t_j \\ \hat{\theta}_i &= \hat{\theta}_i(t_j^+), \ t \in (t_j, t_{j+1}] \end{aligned} \tag{41}$$

The other parameters follows from (44). Uniformly in the simulation, the initial values of states are set as $x_1(0) = 2$, $x_2(0) = 2$, $x_3(0) = 2$, $\hat{\theta}_1(0) = \hat{\theta}_2(0) = \hat{\theta}_3(0) = 0$. The minimum calculation period of simulation is set as 0.01s. Simulation results are recorded for 10s.

The tracking performance of DETC-ST and ETC-CT is shown in Figure 2 and Figure 3. x_1 of both schemes can finally track the reference signal y_d. As is compared in Figure 3, the tracking error z_1 has little difference between two schemes. The tracking performance of ETC-WJ is shown in Figure 4. Because the JVCL problem is not solved, it is difficult to keep the closed-loop system stable. We have to select a very small κ in (40). Figure 5 exhibits the adaptive laws of DETC-ST. Due to the direct adaptive control, all these variables are ultimately bounded. Figure 6 shows the v in (19) and u in (21) of DETC-ST. For the ETC in the CA channel, there are total 525 times signal transmission. The minimum inter-event time equates to 0.01 s. Figure 7 shows the inter-event time of each state in the separate state transmission of DETC-ST. The maximum inter-event occurs in x_2 and equates to 1.56 s. It is observed in the local enlarged view that the transmission of the other states occurs during the inter-event time of each state. The proposed mechanism of separate state transmission works well. Figure 8 shows the inter-event time of ETC-CT. The number of total triggering times is 385 and the maximum inter-event time is 0.18 s. Table 1 presents the quantified performance metrics. Although the occupancy rate of the SC channel in Figure 7 is more than that in Figure 8, only the bandwidth of 1 state is required for DETC-ST, whereas at least the bandwidth of 4 states is required for ETC-CT. This is advantage of the proposed scheme.

Table 1. Performance Metrics.

Indexes	DETC-ST	ETC-CT	ETC-WJ
MTE $\cdot z_1$	0.1014	0.1177	
MCI $\cdot v$	18.6012	20.45540	Difficult to ensure
MCI $\cdot u$	13.3154	15.5457	closed-loop system stability
MAX $\cdot t$	1.56 s	0.18 s	

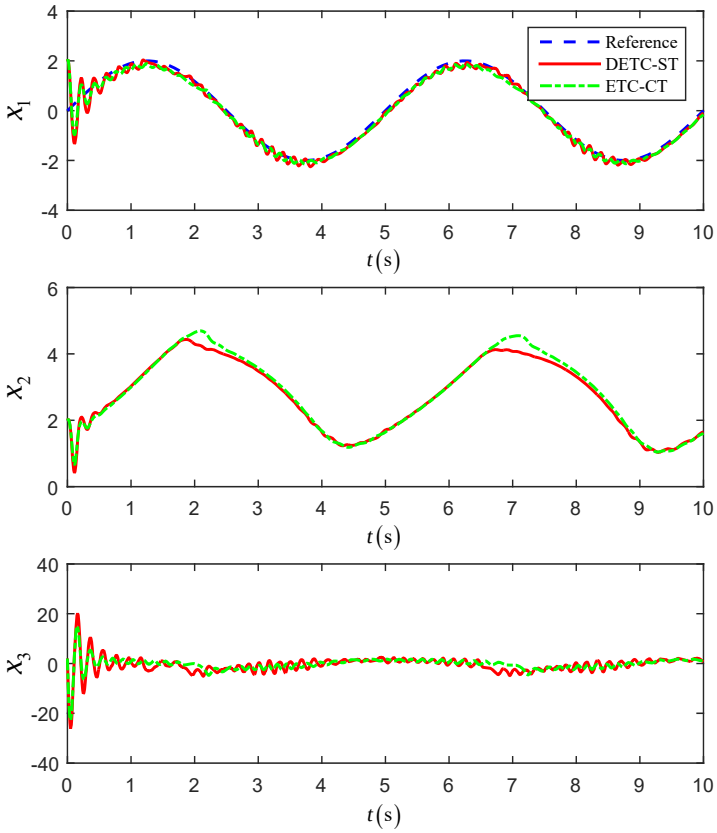

Figure 2. x_1, x_2 and x_3 in DETC-ST and ETC-CT.

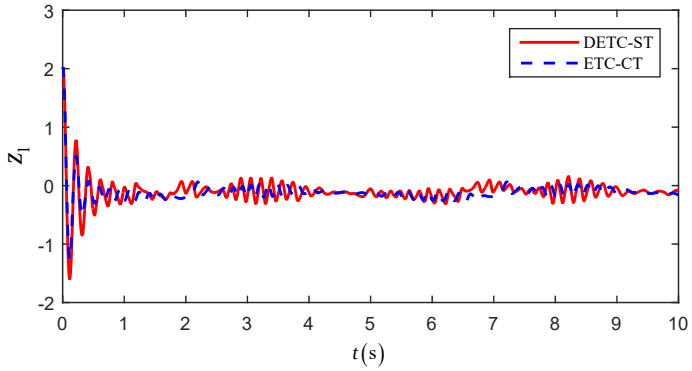

Figure 3. z_1 in DETC-ST and ETC-CT.

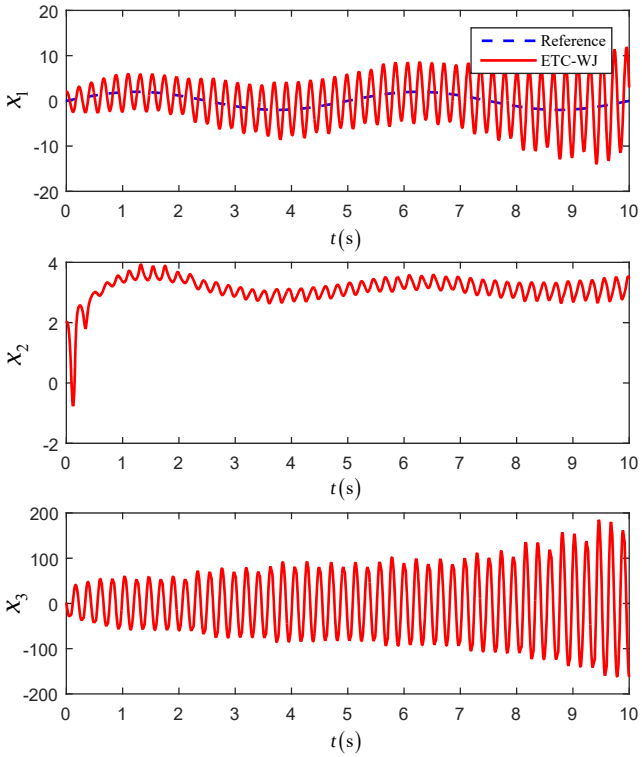

Figure 4. x_1, x_2 and x_3 in ETC-WJ.

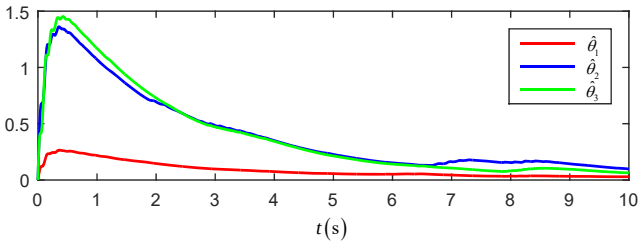

Figure 5. $\hat{\theta}_1$, $\hat{\theta}_2$ and $\hat{\theta}_3$ in DETC-ST.

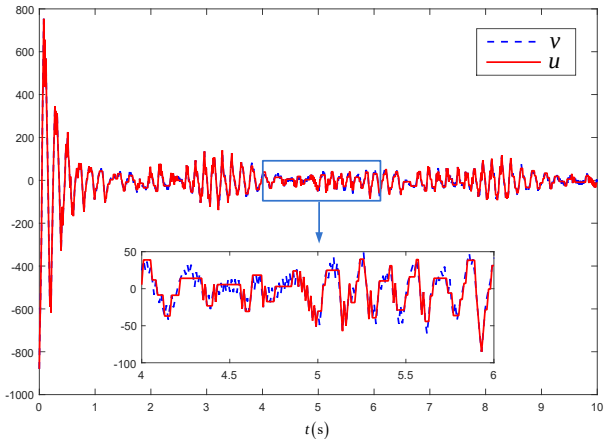

Figure 6. v and u in DETC-ST.

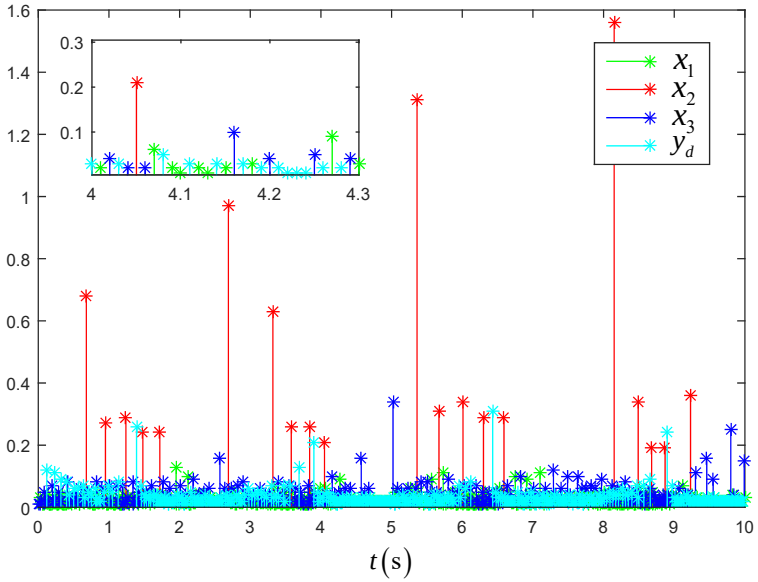

Figure 7. Inter-event time of x_1, x_2, x_3 and y_d in DETC-ST.

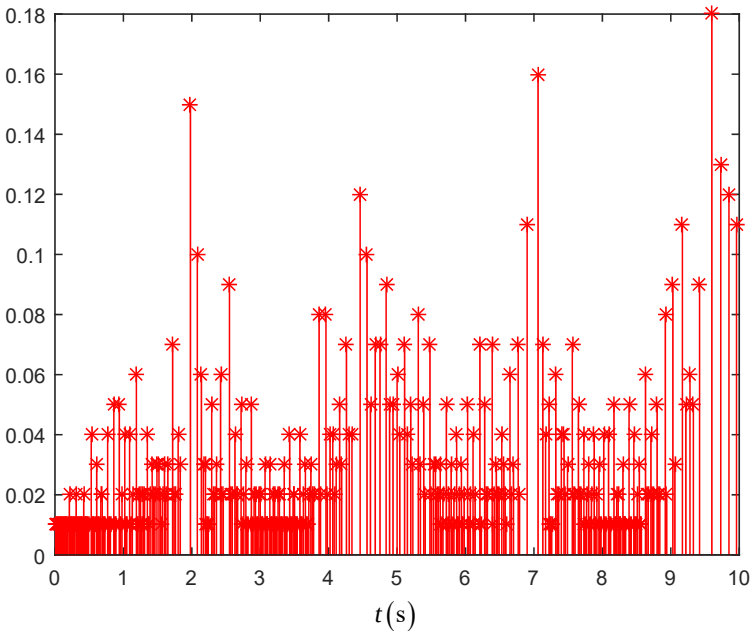

Figure 8. Inter-event time in ETC-CT.

To further analyze the engineering practicability of the algorithm, a brush dc motor driving a one-link robot manipulator system shown in Figure 9 is selected for simulation analysis. The mathematical model of this system is (42).

$$\begin{aligned} \Theta\ddot{q} + N\dot{q} + \sigma\sin(q) + N(\dot{q}I)^2 &= I \\ L\dot{I} &= V - RI - \Gamma_B\dot{q} + Rs^2\sin(I) \end{aligned} \tag{42}$$

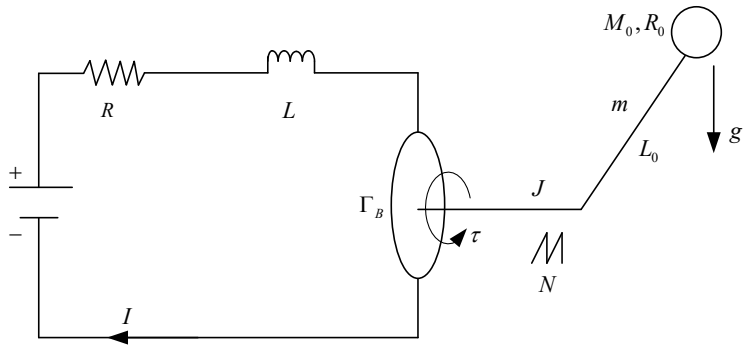

Figure 9. A brush dc motor driving a one-link robot manipulator.

The physical meanings and specific values of each parameter are described in [34], and will not be repeated here. Furthermore, (42) can be rewritten as (43).

$$\begin{aligned}
\dot{x_1} &= x_2 + \sin(t) \\
\dot{x_2} &= -\frac{\sigma}{\Theta}\sin(x_1) - \frac{N}{\Theta}x_2 + \frac{1}{\Theta}x_3 - \frac{N}{\Theta}(x_2x_3)^2 + \sin(0.5t) \\
\dot{x_3} &= \frac{1}{L}u - \frac{R}{L}x_3 - \frac{\Gamma_B}{L}x_2 + \frac{R}{L}x_2^2\sin(x_3) + \sin(0.4t)
\end{aligned} \tag{43}$$

The parameters are set with

$$\begin{aligned}
&k_1 = 15, k_2 = 0.6, k_2 = 0.9, b_1 = b_2 = b_3 = 10, \\
&\lambda_1 = 0.8, \lambda_2 = 10, \lambda_3 = 0.6, \sigma_1 = 0.6, \sigma_2 = 11, \\
&\sigma_3 = 10, \mu_v = 0.2, \mu_u = 0.4, ts = 0.1s
\end{aligned} \tag{44}$$

The reference signal is selected as $y_d = 0.3(\sin(t) + \sin(2t))$. The initial conditions are $x_1(0) = 0.2$, $x_2(0) = 0.2$, $x_3(0) = 0.2$, $\hat{\theta}_1(0) = 0, \theta_2(0) = 0, \theta_3(0) = 0$. Figure 10 to Figure 15 show the simulation results. Figure 10 and Figure 11 show the state and error variation curves under the DETC-ST control strategy. It can be seen that the error is bounded. Figure 12 shows the variation curve of the adaptive law, and Figure 13 shows the variation of control input under event-triggered conditions. Figure 14 and Figure 15 show the interval-times of the SA channel and CA channel. From the above simulation results, it can be seen that the control strategy proposed in this paper is feasible for the engineering practical model.

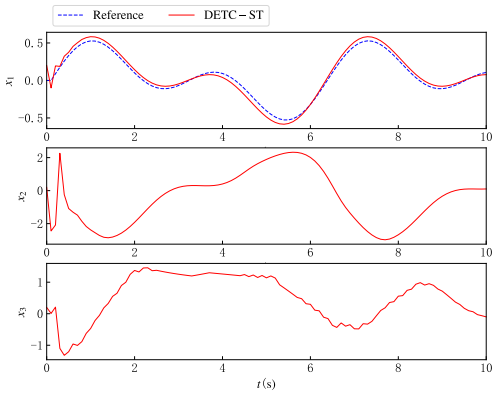

Figure 10. x_1, x_2 and x_3 in DETC-ST.

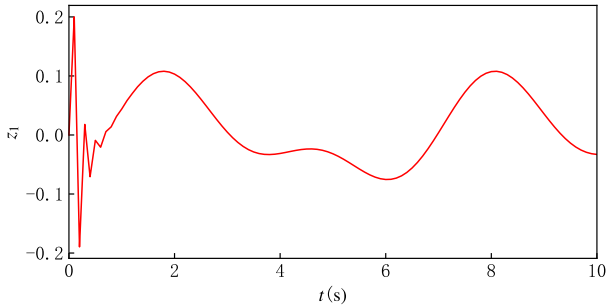

Figure 11. Tracking errror z_1 in DETC-ST.

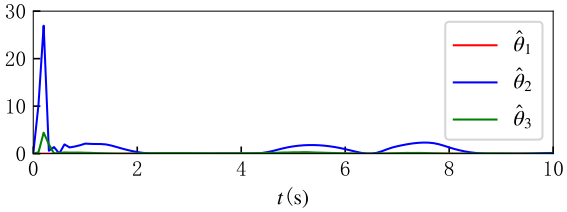

Figure 12. $\hat{\theta}_1$, $\hat{\theta}_2$ and $\hat{\theta}_3$ in DETC-ST.

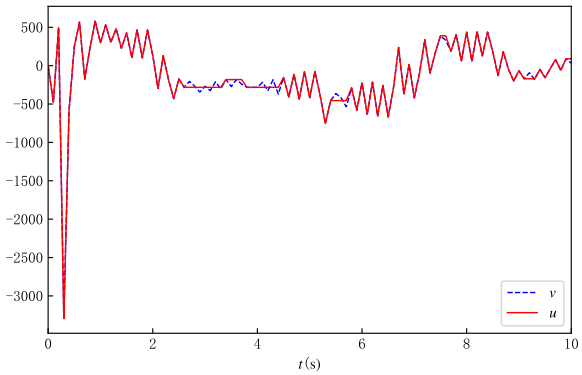

Figure 13. v and u in DETC-ST.

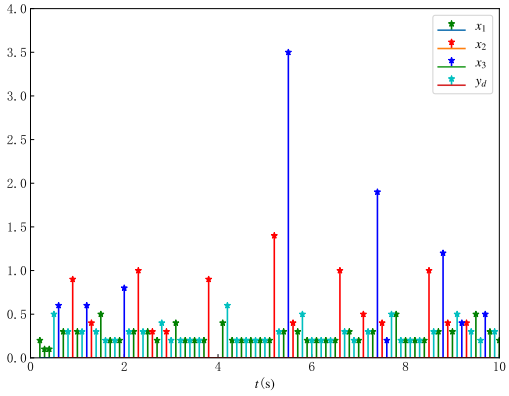

Figure 14. Inter-event time of x_1, x_2, x_3 and y_d in DETC-ST.

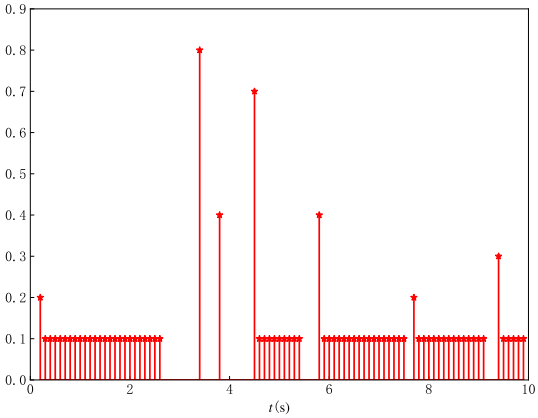

Figure 15. Inter-event time in CA channel.

6. Conclusion

This paper develops a novel method to deal with the JVCL problem in ETC, namely to construct the undetermined virtual control laws which are not involved in the controller. The analysis and design are much easier than the existing researches. A novel event-triggered mechanism is developed by fabricating a cumulative triggering condition, where the state are separately transmitted. This mechanism can save more bandwidth of transmission than the traditional ETC with clustered signal transmission. Furthermore, we conduct a rigorous mathematical proof of the minimum inter-event time of state transmission and the ultimate boundedness of all the tracking errors. Simulation verifies the advantages of the proposed scheme. Nevertheless, the proposed scheme leaves an unsolved problem. As is shown in (19), $\xi_i(t_{j^i})$ must be transmitted along with $x_i(t_{j^i})$. That means $\hat{\theta}_i$ must be calculated in the level of sensors, which increases the computational burden. To solve this problem, we will investigate the adaptive laws co-located with the controller in the future work.

Acknowledgments

This work is partially supported by the Natural Science Foundation of China (No. 52204404, No. 52101375, No. U24A6008), the Hebei Province Natural Science Fund (No. E2024203179, E2022203088), the Science and Technology Project of Hebei Education Department (No. BJ2025114), and the Innovation Capacity Enhancement Program of Hebei Province (No. 24461901D).

Author's contribution

Conceptualization, Yingjie Deng; software, Yingjie Deng, Fangcheng Liu; validation, Tao Ni; formal analysis, Fangcheng Liu; writing—original draft preparation, Fangcheng Liu, Yingjie Deng; writing—review and editing, Fubo Li, Yifei Xu, Tao Ni, Dingxuan Zhao; supervision, Yifei Xu; funding acquisition, Dingxuan Zhao. All authors have read and agreed to the published version of the manuscript.

Conflicts of interests

The authors declared that they have no conflicts of interests.

References

[1] Zhang J, Li S, Ahn CK, Xiang Z. Decentralized event-triggered adaptive fuzzy control for nonlinear switched large-scale systems with input-delay via command-filtered backstepping. *IEEE Trans. Fuzzy Syst.* 2021, 30(6):2118–2123.

[2] Xiong Y, Xiang Z. Fuzzy adaptive output feedback fault-tolerant control for nonlinear switched large-scale systems with sensor faults. *IEEE Syst. J.* 2021, 16(3):3782–3793.

[3] Wen G, Ge SS, Tu F. Optimized backstepping for tracking control of strict-feedback systems. *IEEE Trans. Neural Netw. Learn. Syst.* 2018, 29(8):3850–3862.

[4] Wang M, Wang C. Learning from adaptive neural dynamic surface control of strict-feedback systems. *IEEE Trans. Neural Netw. Learn. Syst.* 2015, 26(6):1247–1259.

[5] Chen B, Liu XP, Ge SS, Lin C. Adaptive fuzzy control of a class of nonlinear systems by fuzzy approximation approach. *IEEE Trans. Fuzzy Syst.* 2012, 20(6):1012–1021.

[6] Chen B, Liu K, Liu X, Shi P, Lin C, *et al.* Approximation-based adaptive neural control design for a class of nonlinear systems. *IEEE Trans. Cybern.* 2014, 44(5):610–619.

[7] Zhou Q, Li H, Wu C, Wang L, Ahn CK. Adaptive fuzzy control of nonlinear systems with unmodeled dynamics and input saturation using small-gain approach. *IEEE Trans. Syst. Man Cybern.: Syst.* 2017, 47(8):1979–1989.

[8] Tong S, Li Y, Sui S. Adaptive fuzzy tracking control design for SISO uncertain nonstrict feedback nonlinear systems. *IEEE Trans. Fuzzy Syst.* 2016, 24(6):1441–1454.

[9] Tong S, Min X, Li Y. Observer-based adaptive fuzzy tracking control for strict-feedback nonlinear systems with unknown control gain functions. *IEEE Trans. Cybern.* 2020, 50(9):3903–3913.

[10] Li Y, Li K, Tong S. Finite-time adaptive fuzzy output feedback dynamic surface control for MIMO nonstrict feedback systems. *IEEE Trans. Fuzzy Syst.* 2019, 27(1):96–110.

[11] Chen B, Zhang H, Liu X, Lin C. Neural observer and adaptive neural control design for a class of nonlinear systems. *IEEE Trans. Neural Netw. Learn. Syst.* 2018, 29(9):4261–4271.

[12] Liu Z, Shi P, Chen B, Lin C. Control design for uncertain switched nonlinear systems: adaptive neural approach. *IEEE Trans. Syst. Man Cybern.: Syst.* 2021, 51(4):2322–2331.

[13] Deng Y, Ni T, Wang J. Event-triggered compound learning tracking control of nonstrict-feedback nonlinear systems in sensor-to-controller channel. *Nonlinear Dyn.* 2021, 106:2259–2276.

[14] Liu Y, Zhu Q. Adaptive neural network asymptotic tracking control for nonstrict feedback stochastic nonlinear systems. *Neural Networks* 2021, 143:283–290.

[15] Wang A, Liu L, Qiu J. Event-triggered adaptive fuzzy output-feedback control for nonstrict-feedback nonlinear systems with asymmetric output constraint. *IEEE Trans. Cybern.* 2020, 52(1):712–722.

[16] Liu Y, Zhu Q, Zhao N. Fuzzy approximation-based adaptive finite-time control for nonstrict feedback nonlinear systems with state constraints. *Inf. Sci.* 2021, 548:101–117.

[17] Wang H, Xu K, Qiu J. Event-triggered adaptive fuzzy fixed-time tracking control for a class

of nonstrict-feedback nonlinear systems. *IEEE Trans. Circuits Syst. I, Reg. Papers.* 2021, 68(7):3058–3068.

[18] Wang Y, Duan G, Li P. Event-triggered adaptive sliding mode control of uncertain nonlinear systems based on fully actuated system approach. *IEEE Trans. Circuits Syst. II Express Briefs.* 2024, 71:2749–2753.

[19] Guo Z, Ren H, Li H, Zhou Q. Adaptive-critic-based event-triggered intelligent cooperative control for a class of second-order constrained multiagent systems. *IEEE Trans. Artif. Intell.* 2023, 4:1654–1665.

[20] Sui S, Shen D, Tong S, Chen CLP. State-observer-based adaptive fuzzy event-triggered formation control for nonlinear multiagent system. *IEEE Trans. Emerging Top. Comput. Intell.* 2024, 8:3327–3338.

[21] Fei Z, Wang X, Yu J. Reliable control for vehicle active suspension systems under event-triggered scheme with frequency range limitation. *IEEE Trans. Syst. Man Cybern.: Syst.* 2021, 51(3):1630–1641.

[22] Li H, Zhang Z, Yan H, Xie X. Adaptive event-triggered fuzzy control for uncertain active suspension systems. *IEEE Trans. Cybern.* 2019, 49(12):4388–4397.

[23] Huo X, Karimi HR, Zhao X, Wang B, Zong G. Adaptive-critic design for decentralized event-triggered control of constrained nonlinear interconnected systems with an identifier-critic framework. *IEEE Trans. Cybern.* 2020, 52(8):7478–7491.

[24] Guo X, Yan W, Cui R. Event-triggered reinforcement learning-based adaptive tracking control for completely unknown continuous-time nonlinear systems. *IEEE Trans. Cybern.* 2020, 50(7):3231–3242.

[25] Li W, Xie Z, Zhao J, Wong PK. Velocity-based robust fault tolerant automatic steering control of autonomous ground vehicles via adaptive event triggered network communication. *Mech. Syst. Sig. Process.* 2020, 143:106798.

[26] Cao L, Zhou Q, Dong G, Li H. Observer-based adaptive event-triggered control for nonstrict-feedback nonlinear systems with output constraint and actuator failures. *IEEE Trans. Syst. Man Cybern.: Syst.* 2021, 51(3):1380–1391.

[27] Xing L, Wen C, Liu Z, Su H, Cai J. Event-triggered adaptive control for a class of uncertain nonlinear systems. *IEEE Trans. Autom. Control.* 2017, 62(4):2071–2076.

[28] Wang L, Chen CLP. Reduced-order observer-based dynamic event-triggered adaptive NN control for stochastic nonlinear systems subject to unknown input saturation. *IEEE Trans. Neural Netw. Learn. Syst.* 2021, 32(4):1678–1690.

[29] Deng Y, Zhang X, Im N, Zhang G, Zhang Q. Model-based event-triggered tracking control of underactuated surface vessels with minimum learning parameters. *IEEE Trans. Neural Netw. Learn. Syst.* 2020, 31(10):4001–4014.

[30] Deng Y, Zhang X, Zhang G, Han X. Adaptive neural tracking control of strict-feedback nonlinear systems with event-triggered state measurement. *ISA Trans.* 2021, 117:28–39.

[31] Wang W, Li Y, Tong S. Neural-network-based adaptive event-triggered consensus control of nonstrict-feedback nonlinear systems. *IEEE Trans. Neural Netw. Learn. Syst.* 2021,

32(4):1750–1764.

[32] Li Y, Yang G. Observer-based fuzzy adaptive event-triggered control co-design for a class of uncertain nonlinear systems. *IEEE Trans. Fuzzy Syst.* 2018, 26(3):1589–1599.

[33] Wang M, Wang Z, Chen Y, Sheng W. Adaptive neural event-triggered control for discrete-time strict-feedback nonlinear systems. *IEEE Trans. Cybern.* 2020, 50(7):2946–2958.

[34] Zhang J, Niu B, Wang D, Wang H, Duan P, *et al.* Adaptive neural control of nonlinear nonstrict feedback systems with full-state constraints: a novel nonlinear mapping method. *IEEE Trans. Neural Netw. Learn. Syst.* 2023, 34(2):999–1007.